Adsorption of Hg(II) Ions from Aqueous Solution by Thiosemicarbazide-modified Cellulose Adsorbent

Jiahao Jiang and Xiwen Wang *

A highly selective cellulose-based adsorbent for mercury [(Hg)II] ion was prepared and characterized using Fourier-transform infrared spectroscopy, X-ray diffraction, thermogravimetric analysis, X-ray photoelectron spectrometry, elemental analysis, and scanning electron microscopy. The results showed that functional thiosemicarbazide-grafted cellulose achieved equilibrium adsorption in 120 min, and the adsorbents had a Hg(II) ion removal rate of approximately 98.5% at a pH of 5.0. The adsorption kinetics fit the pseudo-second-order model, which indicated that the adsorption was a chemical process. Additionally, the adsorption isotherm data showed a best fit with the Langmuir isotherm model, with a maximum Hg(II) ion adsorption capacity of 331.1 mg/g. This adsorbent had a good selectivity for Hg(II) during competitive adsorption.

Keywords: Cellulose; Thiosemicarbazide; Chemical modification; Adsorption; Hg(II)

*Contact information: School of Light Industry and Engineering, State Key Lab of Pulp and Paper Engineering, South China University of Technology, 381 Wushan Road, Guangzhou 510640, Guangdong, People's Republic of China; *Corresponding author: wangxw@scut.edu.cn*

INTRODUCTION

Large amounts of wastewater are generated and discharged globally due to the continuous development of the textile, plastic, printing, and paper industries. This industrial wastewater contains many heavy metal ions, such as mercury, copper, cadmium, and palladium, which compose the principal metallic pollution caused by industrial production. Because they are not biodegradable, once these heavy metal ions are released into the environment they pollute the environment and destroy the ecology. They can also accumulate through entering the food chain, causing serious and sometimes fatal health disorders to humans, including various cancers (Fu and Wang 2011; Salman *et al*. 2015; Lofrano *et al*. 2016; Zhao *et al*. 2018).

Over the past several years, some common techniques have been utilized to remove heavy metal ions from industrial wastewater. These include chemical precipitation (Zhang *et al.* 2016; Gao *et al.* 2018), ion exchange (Khoiruddin *et al.* 2017; Andrzej *et al.* 2018), functionalized membrane (da Silva *et al*. 2016; Khoiruddin *et al.* 2017; Yang *et al.* 2018; Barros *et al*. 2018), ion flotation technique (Xu *et al.* 2017; Yenial and Bulut 2017; Micheau *et al*. 2018), and electrochemical treatment (Kabdaşlı *et al*. 2009; Ali *et al.* 2011). Mercury ion is one of the most hazardous heavy metal ions in wastewater, so these techniques have also been developed to remove mercury ions and have achieved great results (Hou *et al*. 2013; Oehmen *et al.* 2014; Xia *et al.* 2017). Although these techniques can yield positive achievement, they have disadvantages, including high cost, long duration, low sensitivity and stability, susceptibility to contamination, and secondary environmental pollution. Adsorption for heavy metal ion removal yields less environmental pollution and has a high removal efficiency, with additional advantages of

lower cost and portable operation (Yu *et al.* 2014). Meanwhile, various adsorbents, a wide range of source materials, and reusability are also among the important factors that make adsorption one of the most common techniques in the treatment of industrial wastewater (Nayab *et al*. 2014; Yan *et al*. 2014).

Previous studies have examined functionalized adsorbent preparation techniques, which offer flexibility in design and operation and in many cases facilitate the reacquisition of the precious metal ions, yielding additional economic value (Hoai *et al*. 2010). Activated carbon (AC) adsorbents (Hadi *et al*. 2015; Largitte and Pasquier 2016; Park and Lee 2018), carbon nanotubes (CNTs) (Wang *et al*. 2015; Oyetade *et al*. 2017; Zhang *et al*. 2017), and functionalized chitosan (Kheirandish *et al.* 2017; Dinu *et al*. 2018; Mousavi *et al*. 2018) are widely used in the removal of heavy metal contaminants. Bioadsorbents, such as fungi (Yusuf and Tekin 2017; Pourkarim *et al.* 2017), dead biomass (Cheng *et al*. 2017), and bacteria (Qian and Zhan 2016; Manasi *et al.* 2018), are also widely used.

The application of cellulose-based adsorbents for metal ion remediation and wastewater purification has received widespread attention in recent years, and it has the advantages of large surface area, strong mechanical properties, and being biodegradable. Most importantly, the chemically active hydroxyl enhances the adsorption capacity (Lindh *et al.* 2016; Huang *et al.* 2017). Because of the distinctive properties of cellulose, many researchers have attempted to develop functionalized cellulose materials (Hokkanen *et al.* 2016).

There are many methods to functionalize cellulose materials, such as lipidization (Spinella *et al.* 2016; Gan *et al.* 2017), etherification (Abdel-Halim *et al.* 2015; Karatas and Arslan 2016;), graft copolymerization (Deng *et al*. 2016; Sun *et al*. 2018a), and oxidization (Li *et al.* 2015, 2017; Beheshti Tabar *et al.* 2017). Oxidization is one of the most common techniques for cellulose-based material activation (Siller *et al.* 2015; Chen and van de Ven 2016; Cheng *et al.* 2016; Biliuta and Coseri 2016). In all oxidation reactions, the periodate can selectively oxidize the C2-C3 glucose molecule into two aldehyde groups by cleaving the glucopyranoside between them. This behavior allows for further cellulose modification while maintaining the main morphological structure and original properties of cellulose (Yang *et al.* 2015; Azzam *et al.* 2015; Tian and Jiang 2017).

In this study, thiosemicarbazide-modified cellulose (TSC) for Hg(II) selective removal was prepared, and Hg(II) adsorption using the TSC was conducted. The structure and morphology of TSC were characterized *via* Fourier-transform infrared spectroscopy (FTIR), X-ray diffraction (XRD), elemental analysis, and scanning electron microscopy (SEM). The thermodynamic properties were characterized using thermogravimetric analysis. The factors influencing adsorption behavior, including pH, reaction time, and aqueous solution concentration, were also investigated and optimized. The adsorption kinetic parameters of the Hg(II) removal were calculated, and the selectivity of TSC was also evaluated.

EXPERIMENTAL

Materials

Native cellulose extracted from palm wood was collected from the China National Tobacco Corporation (Beijing, China) and washed with deionized water after treatment in 5% (v/v) HCl. Then, the cellulose was oven-dried at 80 °C until reaching a constant weight. Sodium periodate, thiosemicarbazide, hydroxylamine hydrochloride, nitric acid, sodium

hydroxide, and mercury chloride ($HgCl_2$) were purchased from Guangzhou Chemical Reagent Factory (Guangzhou, China). Nitric acid was used after dilution, and the rest of the chemicals were used as received.

Preparation of thiosemicarbazide-modified cellulose

The Hg(II) ion adsorption cellulose was synthesized through a wet chemical process in an aqueous medium according to the following stepwise procedure. First, 1 g of the pretreated cellulose was dispersed into 100 mL of deionized water; 6 mmol sodium periodate per gram of cellulose was used to oxidize the cellulose. Then, the mixture was gently shaken for 6 h at 40 °C in the dark. Next, it was mixed with 10 mL of 10% aqueous ethylene glycol solution, and the mixture was shaken for 30 min to stop the oxidation reaction. After the reaction was over, oxidized cellulose was removed *via* filtration, dialysis, and centrifuging. Finally, the cellulose was washed with deionized water and dispersed. A special reaction between hydroxylamine hydrochloride and oxidized cellulose was conducted to determine the content of the aldehyde groups (Veelaert *et al*. 1997). The aldehyde content was calculated using Eq. 1,

$$\textit{Aldehyde Substitution Degree} = \frac{c\,(V_2 - V_1)\times 162}{m\times 1000}\times 100 \quad (1)$$

where aldehyde substitution degree (%) is the amount of aldehyde per 100 glucoses, V_1 (mL) is the amount of sodium hydroxide for oxidized cellulose, V_2 (mL) is the amount of sodium hydroxide for raw material cellulose, c (mol/L) is the concentration of sodium hydroxide, and m (g) is the weight of the sample.

In the next step, the aqueous wet oxidized cellulose was mixed with thiosemicarbazide to graft the thiourea group onto cellulose. Before mixing with these chemicals, oxidized cellulose was pretreated *via* sonication, and 0.2 g thiosemicarbazide per gram of cellulose was dissolved at 65 °C for 30 min. The mixture was refluxed at 65 °C for 6 h to produce the TSC, and 5 mL of 0.1 M HCl solution was added after the reaction was over. Then, the TSC was removed *via* filtration and washed with deionized water. A special reaction was conducted to determine the amino group content. At 30 °C, 100 mg of sample was dispersed in deionized water, which changed the pH to 3.0. Sodium hydroxide solution was slowly titrated until the pH reached 12.0, and the changes in conductivity were recorded. The amino groups' content was calculated using Eq. 2 (Da Silva Perez *et al*. 2003; Filpponen and Argyropoulos 2010),

$$\textit{Amino Group Content} = \frac{c\,(V_2 - V_1)}{m} \quad (2)$$

where amino group content is in mmol/g, c is the concentration of sodium hydroxide solution, V_1 (mL) is the minimum consumption of sodium hydroxide at the lowest conductivity, V_2 (mL) is the maximum consumption of sodium hydroxide at the lowest conductivity, and m (g) is the weight of the sample.

A schematic of the cellulose modification reactions is shown in Fig. 1.

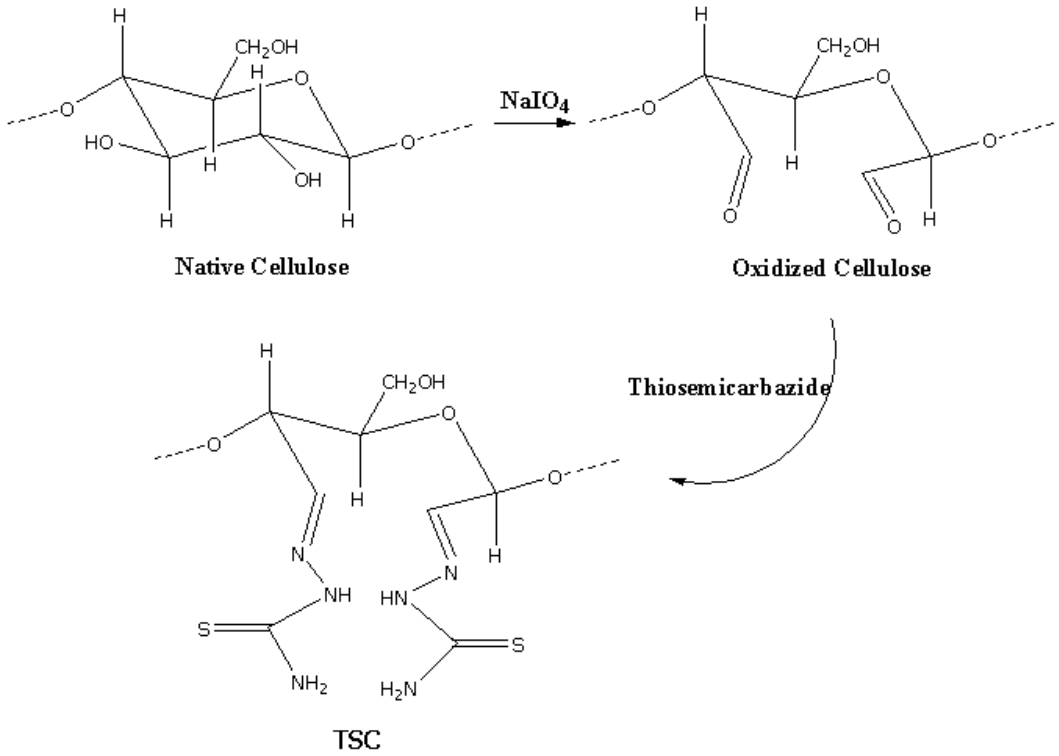

Fig. 1. Synthesis of TSC

Methods

Characterization of samples

A Fourier-transform infrared spectrometer (Bruker VERTEX 70; Bruker Corporation, Billerica, MA, USA) was used to investigate the spectra of the native, oxidized, and modified cellulose. A quantitative analysis of the C, N, O, and S contents of the TSC was performed with an elemental analyzer (Vario EL cube; Elementar, Langenselbold, Germany). An X-ray powder diffractometer (D8 ADVANCE Plus; Bruker Corporation, Billerica, MA, USA) was utilized to investigate the crystallinity of the native, oxidized, and modified cellulose. A scan mode was applied to collect the data for $2\theta = 5°$ to 40°. X-ray photoelectron spectrometry (XPS; ESCALAB 250Xi; Thermo Fisher Scientific Inc., Waltham, MA, USA) was used to analyze the binding energy of the adsorbents for analysis of its elements. A thermogravimetric analysis (TGA; TG 209 F1 Libra®; Netzsch, Selb, Germany) was conducted at a heating rate of 10 °C/min from 40 °C to 600 °C. The metal ion content was determined using inductively coupled plasma optical emission spectrometry (ICP-OES; Optima 5300 DV; PerkinElmer, Waltham, MA, USA). The surface morphology of the samples was examined *via* SEM (EVO 18; Zeiss, Oberkochen, Germany).

Adsorption of Hg(II) on TSC

Effect of initial pH on the adsorption of Hg(II)

The pH value of the solution was one of the key factors that affected the adsorption effectiveness of Hg(II) ions, it not only affected the presence of metal ions but also affected the adsorbent surface charge. In these experiments, 100 mg of TSC was placed in a 250-

mL Erlenmeyer flask containing 200 mL of mercury aqueous solution with a main concentration of 100 mg/L. The adsorption of Hg(II) ions was performed with a pH ranging from 2.0 to 5.0 because metal precipitation interferes with and is indistinguishable from the adsorption phenomenon for pH values up to 7. All of the flasks were shaken using a constant temperature water bath oscillator at a constant shaking rate of 130 rpm for 24 h until adsorption equilibrium. Then, the cellulose was removed by a filter, and the residual Hg(II) ion content was estimated *via* ICP-OES.

The adsorption capacity of Hg(II) ions on TSC and the removal rate of Hg(II) ions were calculated using Eqs. 3 and 4, respectively,

$$q_e = (c_i - c_e)\ \frac{V}{m} \quad (3)$$

$$\textit{Removal Rate}\ (\%) = (c_i - c_e)\ \frac{100}{c_i} \quad (4)$$

where q_e (mg/g) is adsorption capacity, c_i (mg/L) is initial mercury ion concentration, c_e (mg/L) is equilibrium mercury ion concentrations, V (L) is the volume of aqueous solution, and m (g) is the weight of the sample.

Effect of reaction time on the adsorption of Hg(II)

In these experiments, 100 mg TSC was placed in a 250-mL Erlenmeyer flask containing 200 mL of mercury aqueous solution with a main concentration of 100 mg/L, and the adsorption of Hg(II) ions was performed at a pH of 5.0. All of the flasks were shaken using a constant temperature water bath oscillator at a constant rate of 130 rpm with a reaction time from 0 min to 360 min until adsorption equilibrium. Then, the cellulose was removed using a filter, and the residual Hg(II) ion content was estimated *via* ICP-OES.

The adsorption ability of Hg(II) ions on TSC and the removal rate of Hg(II) ions were calculated using Eqs. 3 and 4, respectively.

Effect of solution concentration on the adsorption of Hg(II)

In these experiments, 100 mg TSC was placed in a 250-mL Erlenmeyer flask containing 200 mL of mercury aqueous solution with a main concentration ranging from 50 mg/L to 700 mg/L, and the adsorption of Hg(II) ions was performed at a pH of 5. All of the flasks were shaken using a constant temperature water bath oscillator at a constant rate of 130 rpm for 24 h until adsorption equilibrium. Then, the cellulose was removed by a filter, and the residual Hg(II) ion content was estimated *via* ICP-OES.

The adsorption capacity of the Hg(II) ions on TSC and the removal rate of Hg(II) ions were calculated using Eqs. 3 and 4, respectively.

Selectivity Experiments

The competitive metal ion adsorption studies were performed using a 100 mg sample dispersed in a 250-mL Erlenmeyer flask containing 200 mL of aqueous solution that was mixed together with mercury, lead, cadmium, and copper of an initial concentration of 100 mg/L The adsorption capacity of each metal ion was calculated, and the distribution coefficient (calculated using Eq. 5) was utilized for the selectivity evaluation (Liu *et al.* 2017a; Khan *et al.* 2017),

$$D = [(c_i - c_e) / c_e] \frac{V}{m} \quad (5)$$

where c_i (mg/L) is the initial mercury ion concentration, c_e (mg/L) is the equilibrium mercury ion concentrations, V (L) is the volume of aqueous solution, and m (g) is the weight of the sample.

Desorption Experiments

Desorption experiments on TSC were performed using 0.1 M HNO_3 and 0.1 M HCl solution as the desorption media. The amount of desorbed Hg(II) was measured using ICP-OES.

RESULTS AND DISCUSSION

Characterization of the Modified Cellulose

The results of the oxidation and modification reactions showed that the product yield was approximately 91.2%, and the degree of aldehyde substitution was approximately 46%. The weight loss of cellulose might have been caused by degradation during the chemicals' interaction. The amino group content was approximately 1.15 mmol/g.

The results of the elemental analysis of native cellulose, oxidized cellulose, and modified cellulose are shown in Table 1. After the oxidation and modification of cellulose, there was an obvious increase in the nitrogen and sulfur content, which indicated that the thiosemicarbazide reactive groups were grafted onto the oxidized cellulose.

Table 1. Elemental Analysis of Native, Oxidized, and Modified Cellulose

Cellulose	C (%)	H (%)	O (%)	N (%)	S (%)
Native	41. 23	5. 122	53. 648	-	-
Oxidized	38. 46	4. 977	56. 563	-	-
Modified	39. 13	5. 497	49. 966	3. 19	2. 217

The FTIR results are shown in Fig. 2. The spectra of the native cellulose exhibited diagnostic spectral peaks at approximately 1070 cm^{-1} to 1150 cm^{-1} due to C-O stretching vibrations, 1240 cm^{-1} to 1380 cm^{-1} because of O-H bending, and 3200 cm^{-1} to 3500 cm^{-1} due to O-H stretching. After the oxidation reaction, the adsorption band at 1710 cm^{-1} corresponded to C=O stretching vibration, indicating oxidization of the hydroxyl groups of the cellulose (Koprivica *et al*. 2016; Chen and Ven 2016; Kim *et al.* 2017). After thiosemicarbazide modification, the spectrum showed a new peak at approximately 1670 cm^{-1}, which could have been due to the stretching vibration of C=N of the Schiff base formed between the aldehyde group of the oxidized cellulose and the amino group of the thiosemicarbazide (Monier and Abdel-Latif 2012). In Fig. 2, a peak appears to be present in the TSC spectrum at 1490 cm^{-1}, and the peaks at approximately 767 cm^{-1} and 1230 cm^{-1} were related to the C=S bond. The FTIR spectra indicated that characteristic functional groups were present on the modified cellulose and that TSC was successfully created (Morcali *et al.* 2015; Essawy *et al.* 2016).

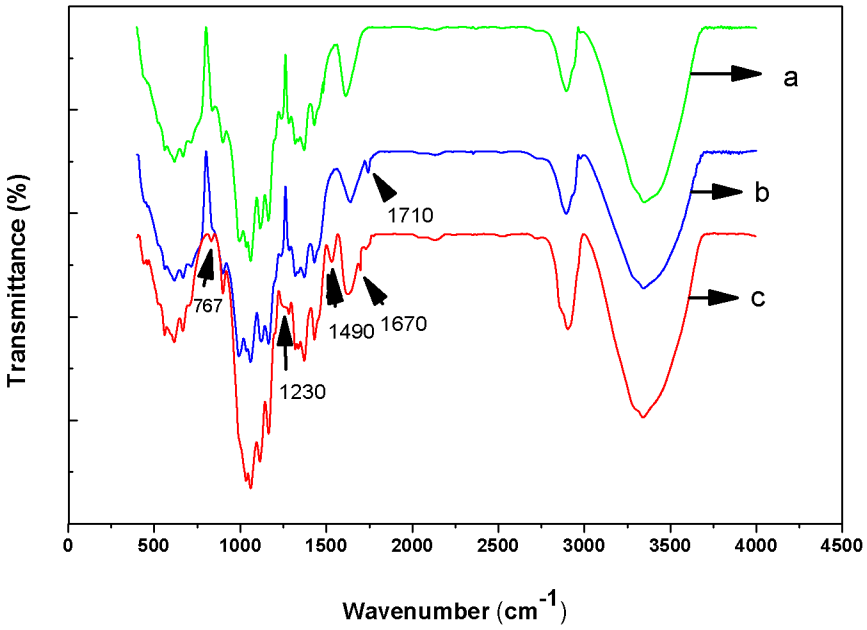

Fig. 2. FTIR spectra of (a) native cellulose, (b) oxidized cellulose, and (c) TSC

The XRD results of the investigation of the crystalline structure are shown in Fig. 3. The native cellulose presented the characteristic crystalline peaks at approximately 16° to 17°, an intense peak at 23°, and a peak at approximately 29°. Meanwhile, there was no noticeable change of characteristic peaks in the XRD patterns of oxidized and modified cellulose (Toba *et al.* 2013). One can make an initial conclusion that the inside aggregate crystalline structures of the oxidized and modified cellulose did not greatly change after the reaction. The crystallinity indices of the different samples are presented in Table 2. The crystallinities of the different cellulose samples were 72.9%, 70.6%, and 67.3% (Segal *et al*. 1959). This phenomenon might have been explained by most hydrogen bonds between the hydroxyls being broken during the oxidization reaction, with the amorphous region created from the subsequent modification reaction (Kim *et al.* 2000).

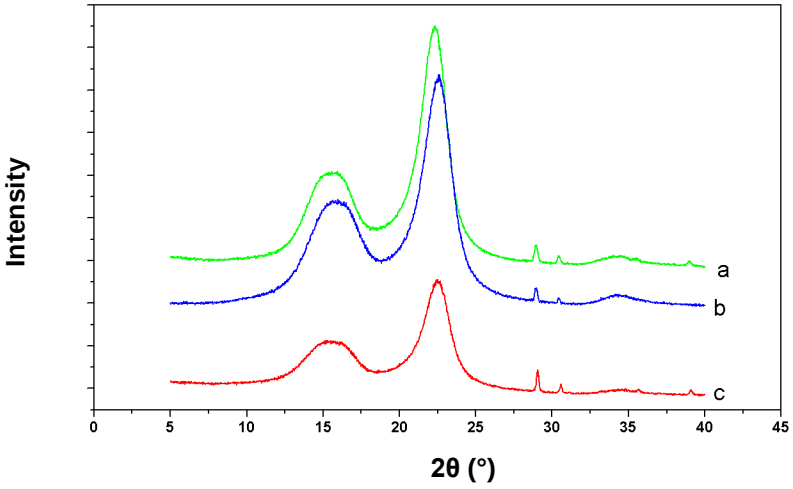

Fig. 3. XRD patterns of (a) native cellulose, (b) oxidized cellulose, and (c) TSC

Table 2. Crystallinity Indices of Different Cellulose Samples

Sample	Native Cellulose	Oxidized Cellulose	TSC
Crystallinity (%)	72.93	70.57	67.31

The native cellulose and modified cellulose were also examined using XPS. Although it simply conducts an analysis of elements on the cellulose surface, XPS provides a valuable indication of changes in the chemical functional groups during the chemical reactions. The XPS survey scans of native cellulose and TSC are presented in Fig. 4. For native cellulose, only two peaks were observed: one at 285.7 eV and another at 533.1 eV, corresponding to C and O, respectively (Banuls-Ciscar *et al.* 2016). However, for the TSC, the XPS spectrum showed a nitrogen adsorption peak at 400.2 eV and the S2p specific peak at approximately 162.4 eV. These results were further evidence for TSC's successful creation (Konshina *et al*. 2016; Ahmad *et al*. 2018).

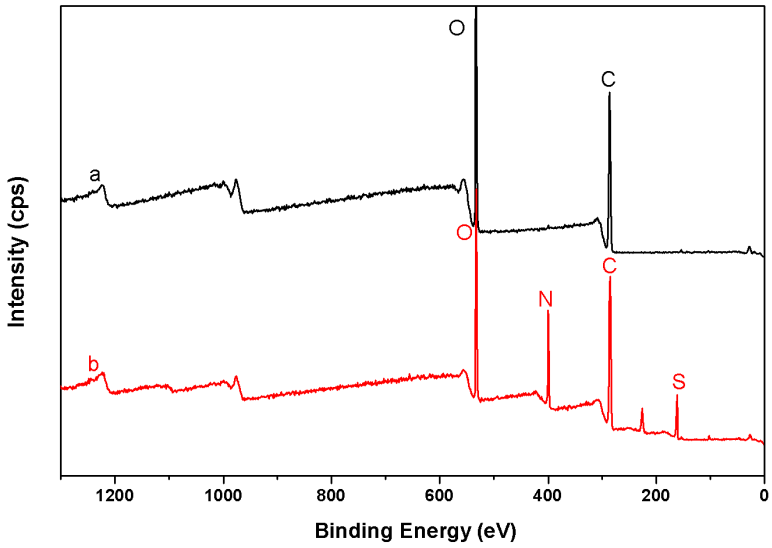

Fig. 4. XPS patterns of (a) native cellulose and (b) TSC

Thermogravimetric analysis was employed to evaluate the thermal stability of the native cellulose, oxidized cellulose, and modified cellulose. The TGA curves are shown in Fig. 5. The thermal degradation temperature of native cellulose was approximately 260 °C. The mass of the native samples decreased while the temperature was below 120 °C due to water evaporation inside the cellulose. Although the samples were dried prior to TGA, some moisture could not be removed because of hydrogen bonding. The thermal degradation temperature of oxidized cellulose was approximately 200 °C; the thermal stability of oxidized cellulose was reduced compared to native cellulose. After cellulose oxidization by sodium periodate, the C_2-C_3 bonds on each glucose unit of the cellulose molecular chains were fractured, which destroyed the six-membered ring structure of the glucose units and led the oxidized cellulose to degrade at a lower temperature. The thermal degradation temperature of modified cellulose was greater than that of oxidized cellulose and was up to 220 °C. This might have been because the thiosemicarbazide functional group grafted onto the oxidized cellulose molecular chains, which lengthened the modified cellulose molecular chains.

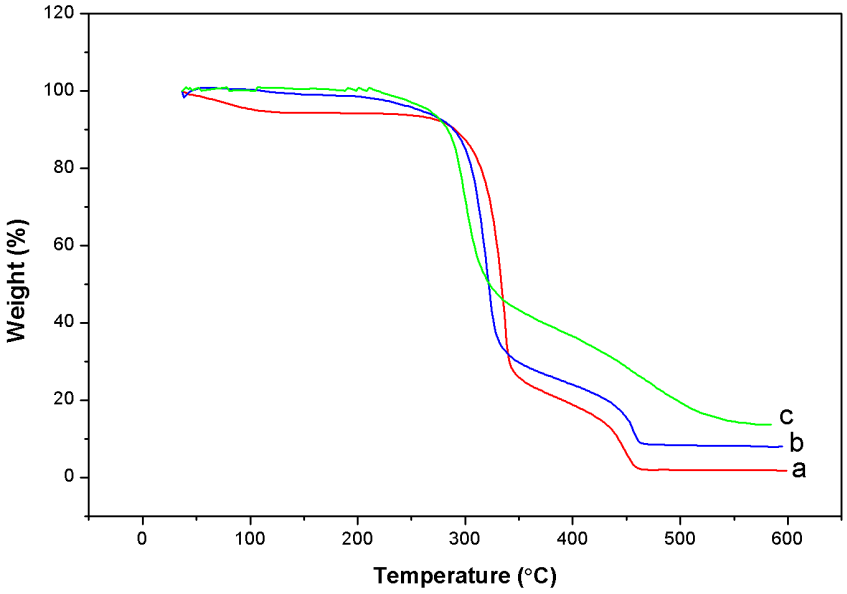

Fig. 5. TGA of (a) native cellulose, (b) oxidized cellulose, and (c) TSC

The SEM results for the native cellulose and TSC are displayed in Fig. 6. As can be easily observed with approximately 500× magnification, the cellulose lengths were approximately several mm, and the widths were approximately 10 µm. Moreover, the native cellulose surface was smooth and had no swelling from dehydration. In contrast, the rough and porous surface of the modified cellulose indicated that after oxidation and thiosemicarbazide modification, functional and active sites were distributed on the cellulose surface, providing greater specific surface area and enhancing the ability to adsorb Hg(II). Meanwhile, the lengths and widths of the cellulose were distributed more evenly, and the widths were slightly reduced to approximately 7.0 µm. This result may have been the reason for chemicals touching the amorphous area of cellulose and causing degradation.

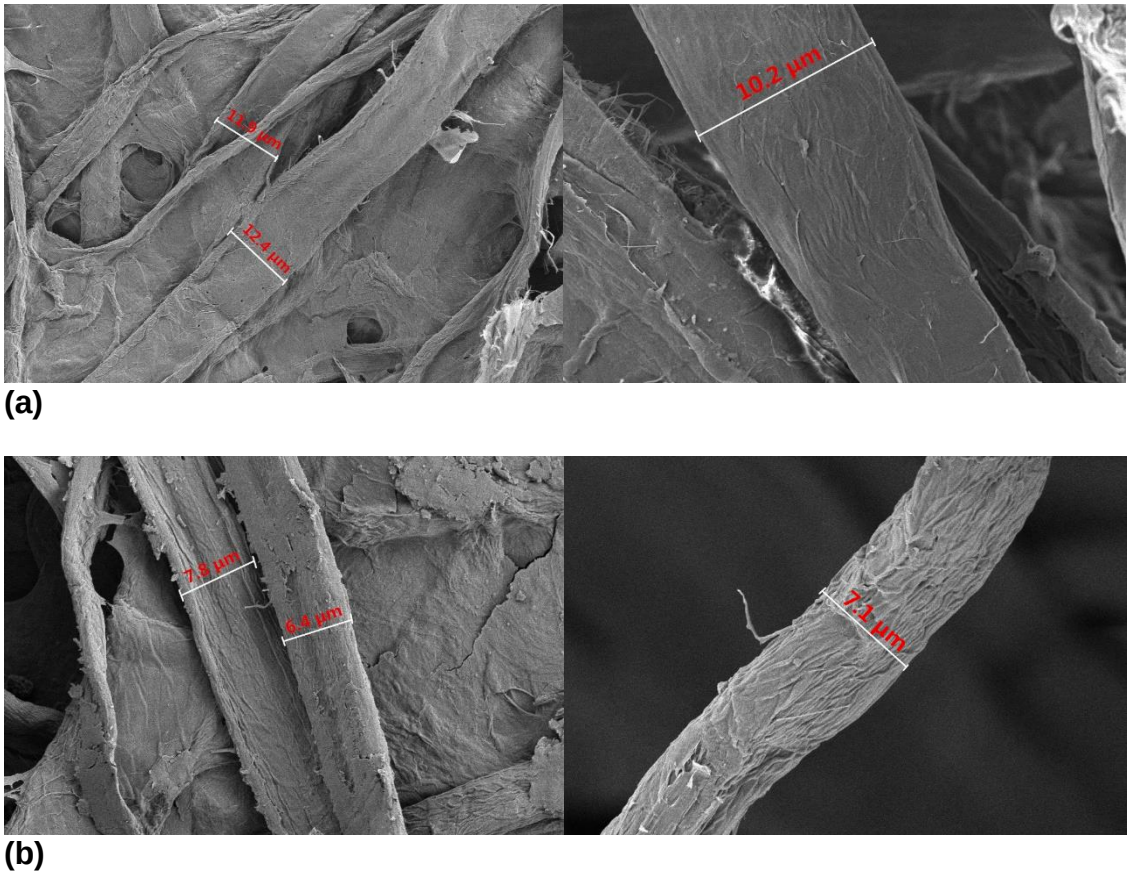

Fig. 6. SEM photos of (a) native cellulose and (b) modified cellulose

Adsorption Properties

Mercury(II) chloride was selected for the Hg(II) solute because it is ionized to $(HgCl)^-$ instead of Hg(II). Then, $(HgCl)^-$ was ionized to Hg(II) and Cl^- through an ionization balance process. When Hg(II) ions were adsorbed by TSC, the decrease of Hg(II) ion concentration in the system promoted the further ionization of $(HgCl)^-$. Therefore, the concentration of $HgCl_2$ could be raised to a higher level without fear of forming a precipitate. Inductively coupled plasma optical emission spectrometry detects the total amount of Hg(II) in the solution; its particular form would not affect the test results.

Effect of pH

Many previous studies have shown that the pH of a solution makes an essential impact in chemical heavy metal ion adsorption experiments (Monier and Abdel-Latif 2013; Guo *et al*. 2016). The pH value range of 2.0 to 5.0 was to determine the effect of the removal of Hg(II) by TSC. Higher pH values could not conduct, because with pH values of 6 and greater the Hg(II) ions would form a precipitate. The adsorption results are shown in Fig. 7. As shown in the adsorption curve, the removal rate of Hg(II) ions clearly increased when raising the pH from 2.0 to 5.0. This trend might have been because the Hg(II) ions adsorption mainly *via* the active sites on the surface of the modified cellulose could coordinate with the heavy metal cation. When pH was low, the quantity of hydrogen ions in the aqueous solution increased, and the majority of the active adsorption functional groups had been protonated. Consequently, the cellulose surface was full of positive

charge, which subsequently weakened the coordination capability between the surface active sites and the Hg(II) ions. With increased pH, the quantity of hydroxide in the aqueous solution also increased, resulting in charge transfer in the carbon-sulfur double bond and the formation of a thioether structure, which subsequently enhanced the Hg(II) adsorption (Motahari *et al*. 2015; Sarkar *et al*. 2016; Zou *et al*. 2017).

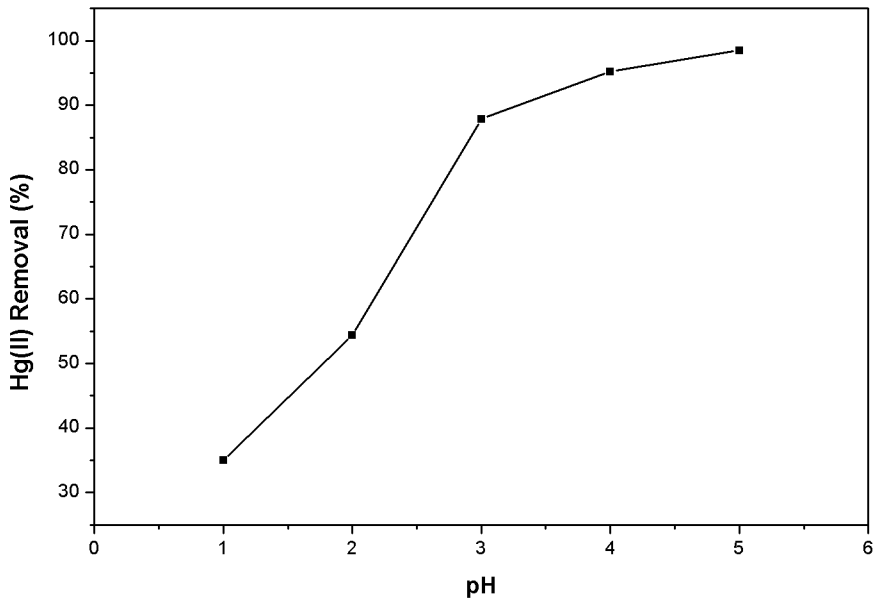

Fig. 7. Effect of pH value on the removal of Hg(II) ions by TSC (initial concentration 100 mg/L, adsorbent 0.5 g/L, shaking rate 130 rpm, 30 °C, and for 24 h)

Adsorption Kinetics

To investigate the time to reach saturation during the adsorption process, the adsorption rate throughout the experiment's duration, and the interaction between the adsorbent and the heavy metal ions, Hg(II) ion adsorption kinetic experiments were conducted at 30 °C and an initial concentration of 100 mg/L from 0 min to 360 min. The results of the adsorption rate throughout the experiment are exhibited in Fig. 8. As is clearly shown in the curve, the adsorption rate continuously decreased with the time elapsed until the adsorption capacity had reached saturation at 176 mg/g after approximately 100 min.

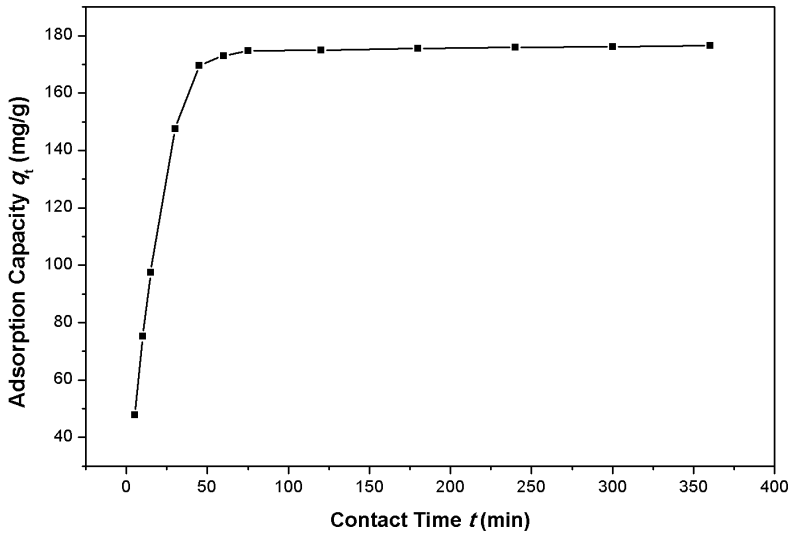

Fig. 8. Effect of contact time on the removal of Hg(II) ions by TSC (initial concentration 100 mg/L, adsorbent 0.5 g/L, pH 5.0, shaking rate 130 rpm, and at 30 °C)

Because there are various functional groups in the TSC, such as N-H and C=S, it is essential to investigate the different possible interaction types. The Hg(II) ion adsorption data were subjected to kinetic adsorption model fitting and analysis for increased comprehension of the adsorption mechanism, and finally determined the limit for the rate that affected the adsorption process (Lee and Kim 2016; Zhu *et al.* 2017; Cruz-Tirado *et al.* 2017).

The most frequently used kinetic equations to describe the uptake kinetic mechanism are the pseudo-first-order equation (Eq. 6) and the pseudo-second-order equation (Eq. 7) (Ho and McKay 1999; Azizian 2004),

$$\ln(q_e - q_t) = \ln q_e - k_1 t \quad (6)$$

$$\frac{t}{q_t} = \frac{1}{k_2 q_e^2} + \frac{t}{q_e} \quad (7)$$

where q_t (mg/g) is the adsorption capacity at time t (min), and k_1 (min^{-1}) and k_2 (g/(mg·min)) are the adsorption rate constants of the pseudo-first-order kinetic model and pseudo-second-order kinetic model.

For both kinetic models, k and q_e are usually calculated by calibrating the linear plots of $\ln(q_e - q_t)$ and t/q_t *versus* t and then comparing the theoretical values with experimental values to evaluate the best kinetic models that fit with the work.

Table 3 lists the constants q_e, k, and R^2, which describe the adsorption mechanism and models. Clearly, the pseudo-second-order equation showed a better match with the experimental data between the experimental and calculated q_e and the high value of R^2 (> 0.999). Furthermore, the better fit of the pseudo-second-order equation signified that the adsorption (Yao *et al*. 2016; Dogan *et al.* 2018; Song *et al.* 2018). Additionally, TSC exhibited a high initial adsorption rate of 22.35 mg/(g·min) for Hg(II), which was greater than those in previous reports (Yao *et al*. 2016). Noticeably, the pseudo-first-order model was not an appropriate model of the adsorption kinetic behavior because of the poor value of R_1^2 (< 0.86).

Table 3. Kinetic Parameters for Hg(II) Adsorption by TSC

Metal Ion	$q_{e.exp}$ (mg/g)	Pseudo-first-order Model			Pseudo-second-order Model		
		q_e (mg/g)	k_1 (min^{-1})	R_1^2	q_e (mg/g)	k_2 (g/(mg•min))	R_2^2
Hg(II)	176.62	177.01	0.05768	0.85475	181.82	6.76×10^{-4}	0.9994

Adsorption isotherms

Two extensively applied adsorption isotherm models, the Langmuir and Freundlich models, are important in explaining the relation between the Hg(II) ions on the adsorbent samples and the initial concentration of the metal ions. These two common isotherm models are formulated as the Langmuir equation (Eq. 8) and the Freundlich equation (Eq. 9) (Yao 2000; Senniappan *et al.* 2016; Taoufik *et al.* 2017),

$$\frac{c_e}{q_e} = (\frac{1}{k_L q_m}) + (\frac{c_e}{q_m}) \quad (8)$$

$$\ln q_e = \ln k_F + \frac{1}{n}(\ln c_e) \quad (9)$$

where q_e (mg/g) is the adsorption capacity of metal ions at equilibrium, c_e (mg/L) is the metal ion concentration of solution at equilibrium, k_L (L/mg) is the Langmuir constant, q_m (mg/g) is the maximum adsorption capacity of the adsorbent, k_F is the Freundlich constant, and $1/n$ is the heterogeneity factor.

Comparing these two adsorption isotherm models in principle, the Langmuir model assumes that the heat of adsorption was constant throughout the adsorption process and that the adsorption process was an isothermal monolayer interaction that was established on adsorbent molecules and metal ions. Meanwhile, the Freundlich model is an isothermal adsorption equation utilized as a semi-empirical formula (Afonso *et al*. 2016; Terdputtakun *et al*. 2017).

The adsorption experiments for isotherm models were conducted at 30 °C, and the results are exhibited in Fig. 9. Clearly, the adsorption capacity continuously increased, but the adsorption rate continuously slowed until reaching equilibrium.

The experimental data were fitted with both the Langmuir and Freundlich isotherms. The results and parameters are listed in Table 4. Clearly, compared with the Freundlich isotherm, the Langmuir isotherm had a better fitness for the equilibrium with $R^2 = 0.992$. This result indicates that adsorption of Hg(II) ions by TSC mainly followed the monolayer adsorption pattern, and the theoretical maximum adsorption capacity was 331.1 mg/g.

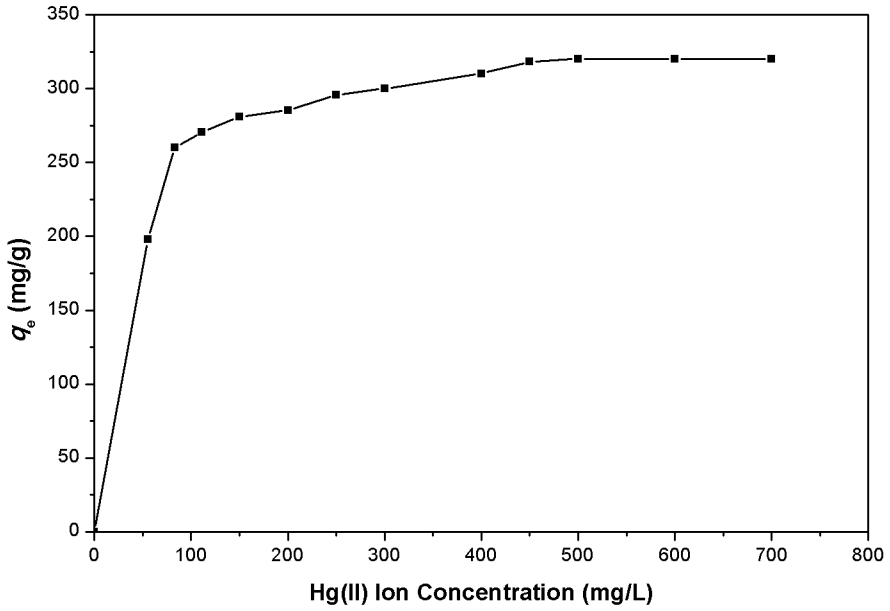

Fig. 9. Adsorption isotherms of Hg(II) ions by TSC (initial concentration 0 mg/L to 700 mg/L, adsorbent 0.5 g/L, pH 5, shaking rate 130 rpm, and at 30 °C)

Table 4. Parameters for Hg(II) Ion Adsorption by TSC According to Different Equilibrium Isotherms

Langmuir Isotherm Parameters			Freundlich Isotherm Parameters		
k_L(L/g)	q_m (mg/g)	R^2	lnk_F	n	R^2
0.0405	331.13	0.992	4.726	5.8	0.91322

The essential characteristic of the Langmuir model can be reflected by the constant R_L, which evaluated the suitability of the adsorption process. It can be calculated as follows in Eq. 10 (Monier *et al*. 2014; Wang *et al.* 2017),

$$R_L = \frac{1}{1 + c_0 k_L} \quad (10)$$

where c_0 is the initial concentration of metal ions in solution. The value of R_L presents the tendency of the isotherm to be unfavorable ($R_L > 1$), linear ($R_L = 1$), favorable ($0 < R_L < 1$), or irreversible ($R_L = 0$). Further, a smaller R_L value predicts greater affinity between the adsorbent and metal ions. The specific values for Hg(II) adsorption by TSC were between 0.034 and 0.308, indicating that TSC is a suitable adsorbent for Hg(II) ions (Tian et al. 2011b; Liu *et al.* 2017b).

The results of Hg(II) ion adsorption on different adsorbents under similar experimental conditions are exhibited in Table 5. The maximum adsorption capacity for Hg(II) of TSC is the greatest among several other adsorbents. The factors affecting the disparity in Hg(II) ion removal were the properties of the different adsorbents.

Table 5. Adsorption Capacities of Hg(II) Ions onto Other Similar Adsorbents

Adsorbent	q_m (mg/g)
Poly(methacrylic acid)-modified cellulose acetate (Tian *et al*. 2011a)	23.8
Activated carbon prepared from agricultural solid waste (Kadirvelu *et al*. 2001)	125
PP-g-AA-TU fibers (Yao *et al*. 2016)	52.02
(SBF-g-SA)-g-PAM (Sun *et al*. 2018b)	178.0
TSC (present study)	331.13

Metal ion competitive adsorption

In this study, it was necessary to consider the selectivity of adsorption of different heavy metal ions by modified adsorbent samples. Table 6 shows the selective separation and distribution coefficient of Hg(II) adsorption on TSC compared with Pb(II), Cd(II), and Cu(II) at a pH of 5.0, with an initial concentrations of 100 mg/L, and at 30 °C. The adsorption capacity of Hg(II) ions was 186.2 mg/g in the case of interference by other heavy metal ions, which indicated an excellent selectivity of Hg(II) by TSC.

The distribution coefficient was calculated by Eq. 5, and the selectivity coefficient that indicated the modified adsorbent's ability to adsorb Hg(II) ions compared to other metal ions is also shown in Table 6. As shown, TSC presented a distribution coefficient for Hg(II) over 50 times greater than for the other heavy metal ions. These results indicated that the functional sites grafted on TSC after the modification reaction can better form complex structures with Hg(II) ions (Chen *et al.* 2018; Wu *et al.* 2018).

Table 6. Selective Adsorption of Hg(II) from Multi-component Mixtures by TSC

Metal	q_e (mg/g)	D (L/g)	Selectivity Coefficient $\beta_{Hg(II)/M^{n+}}$
Hg(II)	186.21	27.01	-
Pb(II)	42.51	0.54	50.02
Cu(II)	39.32	0.49	55.12
Cd(II)	36.12	0.44	61.39

Note: Initial concentration 100 mg/L, adsorbent 0.5 g/L, shaking rate 130 rpm, solution pH 5.0, and at 30 °C

Desorption and reusability of TSC

After measuring the Hg(II) concentration in the desorption medium, the desorption ratios for Hg(II) metal ions using 0.1 M HNO_3 and 0.1 M HCl solutions were 91.3% and 92.6%, respectively. The adsorption capacity of TSC could still reach 85% after five cycles, so there was no particularly notable decrease in the adsorption efficiency of TSC.

Adsorption mechanism

Figure 10 shows the sulfur element (S2p) XPS spectra of TSC before and after Hg(II) adsorption. As shown, the binding energy of the narrow XPS spectrum for S2p was 162.5 eV, which may have been due to the C=S bonds. After adsorption of Hg(II), the S2p binding energy moved to a slightly greater value of 165.4 eV, corresponding to the transfer of electrons from S atoms of -C=S- to Hg(II) (Bai *et al*. 2011; Ding *et al.* 2016). Figure 11 shows the mercury element (Hg4f) XPS spectrum of TSC after adsorption. As shown in the curve, 101.1 eV and 104.9 eV Hg4f binding energies could suggest coordination *via* -C=S- groups, as illustrated in the molecularly modeled schematic in Fig. 12 (Yao *et al*. 2016; Jie *et al.* 2018).

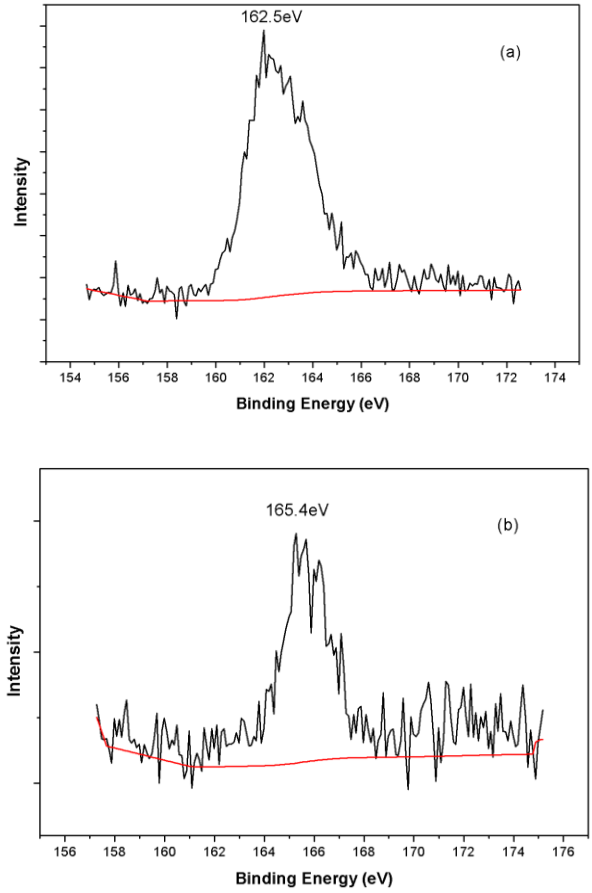

Fig. 10. S2p narrow XPS scan for TSC before (a) and after (b) adsorption of Hg(II) (initial concentration 100 mg/L, adsorbent 0.5 g/L, pH 5.0, shaking rate 130 rpm, and at 30 °C)

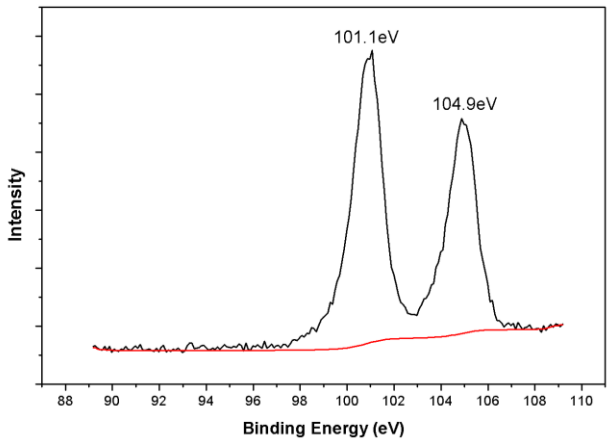

Fig. 11. Hg4f narrow XPS scan for TSC after adsorption of Hg(II) (initial concentration 100 mg/L, adsorbent 0.5 g/L, pH 5.0, shaking rate 130 rpm, and at 30 °C)

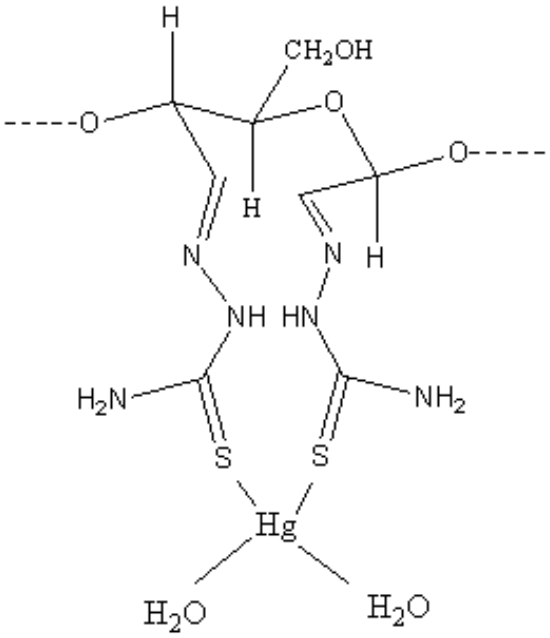

Fig. 12. Proposed model of complexation of Hg(II) with TSC

CONCLUSIONS

1. A novel and functional adsorbent for Hg(II) removal in aqueous solutions was prepared by employing thiosemicarbazide to modify dialdehyde cellulose. The mercapto group on the surface of this derived chelating cellulose could efficiently and effectively adsorb Hg(II) ions with high selectivity.
2. The performance of TSC was investigated by various techniques, and the adsorption properties of Hg(II) ion removal were also studied under different conditions. The adsorption behaviors of modified cellulose were superior to native cellulose both in equilibrium adsorption ability and in adsorption rate.
3. The adsorption kinetics of Hg(II) onto TSC was fast and followed the pseudo-second-order model, which indicated that chemical adsorption occurred during the adsorption process.
4. The Langmuir isotherm model had the best fit with the Hg(II) ion adsorption data through a monolayer adsorption capacity of 331.1 mg/g.
5. The results of the multi-component system adsorption experiments supported the TSC's selectivity toward Hg(II) ions in the presence of interference from other ions.

ACKNOWLEDGMENTS

This work was supported by the National Natural Science Foundation of China (31470608).

REFERENCES CITED

Abdel-Halim, E. S., Alanazi, H. H., and Al-Deyab, S. S. (2015). "Utilization of olive tree branch cellulose in synthesis of hydroxypropyl carboxymethyl cellulose," *Carbohydrate Polymers* 127, 124-134. DOI: 10.1016/j.carbpol.2015.03.037

Afonso, R., Gales, L., and Mendes, A. (2016). "Kinetic derivation of common isotherm equations for surface and micropore adsorption," *Adsorption* 22(7), 963-971. DOI: 10.1007/s10450-016-9803-z

Ahmad, M., Manzoor, K., Ahmad, S., and Ikram, S. (2018). "Preparation, kinetics, thermodynamics, and mechanism evaluation of thiosemicarbazide modified green carboxymethyl cellulose as an efficient Cu(II) adsorbent," *Journal of Chemical & Engineering Data* 63(6), 1905-1916. DOI: 10.1021/acs.jced.7b01008

Ali, I., Khan, T. A., and Asim, M. (2011). "Removal of arsenic from water by electrocoagulation and electrodialysis techniques," *Separation and Purification Reviews* 40(1), 25-42. DOI: 10.1080/15422119.2011.542738

Andrzej, K., Aneta, S., Aleksandra, B., Gil, B., Malgorzata, R., and Zofia, P. (2018). "Effective catalysts for the low-temperature NH_3-SCR process based on MCM-41 modified with copper by template ion-exchange (TIE) method," *Applied Catalysis B: Environmental* S0926337318305861-. DOI: 10.1016/j.apcatb.2018.06.052

Azzam, F., Galliot, M., Putaux, J. L., Heux, L., and Jean, B. (2015). "Surface peeling of cellulose nanocrystals resulting from periodate oxidation and reductive amination with water-soluble polymers," *Cellulose* 22(6), 3701-3714. DOI: 10.1007/s10570-015-0785-x

Azizian, S. (2004). "Kinetic models of sorption: A theoretical analysis," *Journal of Colloid and Interface Science* 276(1), 47-52. DOI: 10.1016/j.jcis.2004.03.048

Bai, L., Hu, H., Fu, W., Wan, J., Cheng, X., Zhuge, L., Xiong, L., and Chen, Q. (2011). "Synthesis of a novel silica-supported dithiocarbamate adsorbent and its properties for the removal of heavy metal ions," *Journal of Hazardous Materials* 195, 261-275. DOI: 10.1016/j.jhazmat.2011.08.038

Banuls-Ciscar, J., Abel, M. L., and Watts, J. F. (2016). "Characterisation of cellulose and hardwood organosolv lignin reference materials by XPS," *Surface Science Spectra* 23(1), 1-8. DOI: 10.1116/1.4943099

Barros, K. S., Scarazzato, T., and Espinosa, D. C. R. (2018). "Evaluation of the effect of the solution concentration and membrane morphology on the transport properties of Cu(II) through two monopolar cation–exchange membranes," *Separation and Purification Technology* 193, 184-192. DOI: 10.1016/j.seppur.2017.10.067

Beheshti Tabar, I., Zhang, X., Youngblood, J. P., and Mosier, N. S. (2017). "Production of cellulose nanofibers using phenolic enhanced surface oxidation," *Carbohydrate Polymers* 174, 120-127. DOI: 10.1016/j.carbpol.2017.06.058

Biliuta, G., and Coseri, S. (2016). "Magnetic cellulosic materials based on tempo-oxidized viscose fibers," *Cellulose* 23(6), 3407-3415. DOI: 10.1007/s10570-016-1082-z

Chen, D., and van de Ven, T. G. M. (2016). "Morphological changes of sterically stabilized nanocrystalline cellulose after periodate oxidation," *Cellulose* 23(2), 1-9. DOI: 10.1007/s10570-016-0862-9

Chen, J., Wang, N., Liu, Y. P., Zhu, J. W., Feng, J. T., Yan, W. (2018). "Synergetic effect in a self-doping polyaniline/TiO_2 composite for selective adsorption of heavy metal ions," *Synthetic Metals* 245, 32-41. DOI: 10.1016/j.synthmet.2018.08.006

Cheng, D., Wen, Y., An, X., Zhu, X., and Ni, Y. (2016). "Tempo-oxidized cellulose nanofibers (TOCNs) as a green reinforcement for waterborne polyurethane coating (wpu) on wood," *Carbohydrate Polymers* 151, 326-334. DOI: 10.1016/j.carbpol.2016.05.083

Cheng, J., Yin, W., Chang, Z., Lundholm, N., and Jiang, Z. (2017). "Biosorption capacity and kinetics of cadmium(II) on live and dead *Chlorella vulgaris*," *Journal of Applied Phycology* 29(1), 211-221. DOI: 10.1007/s10811-016-0916-2

Cruz-Tirado, J. P., Cabanillas, A., Raúl Siche, Espina, J., and Ibarz, A. (2017). "Bleaching of sugar cane juice using a food-grade adsorber resin and explained by a kinetic model describing the variation in time of the content of adsorbate," *Food Science and Technology International* 24(3), 264-274. DOI: 10.1177/1082013217747711

Da Silva, J. R. P., Merçon, F., Costa, C. M. G., and Benjo, D. R. (2016). "Application of reverse osmosis process associated with EDTA complexation for nickel and copper removal from wastewater," *Desalination and Water Treatment* 57(41), 19466-19474. DOI: 10.1080/19443994.2015.1100554

Da Silva Perez, D., Montanari, S., and Vignon, M. R. (2003). "TEMPO-mediated oxidation of cellulose III," *Biomacromolecules* 4(5), 1417-1425. DOI: 10.1021/bm034144s

Deng, F., Zhang, Y., Ge, X., Li, M. C., Li, X., Cho, U. R. (2016). "Graft copolymers of microcrystalline cellulose as reinforcing agent for elastomers based on natural rubber," *Journal of Applied Polymer Science* 133(9). DOI: 10.1002/app.43087

Ding, S., Dong, M., Wang, Y., Chen, Y., Wang, H., and Su, C., and Wang, W. (2016). "Thioether-based fluorescent covalent organic framework for selective detection and facile removal of mercury(II)," *Journal of the American Chemical Society* 138(9), 3031-3037. DOI: 10.1021/jacs.5b10754

Dinu, M. V., Dinu, I. A., Lazar, M. M., and Dragan, E. S. (2018). "Chitosan-based ion-imprinted cryo-composites with excellent selectivity for copper ions," *Carbohydrate Polymers* 186, 140-149. DOI: 10.1016/j.carbpol.2018.01.033

Dogan, O., Bodur, B., and Inan, G. (2018). "Kinetic and thermodynamic studies of Cu(II) adsorption onto calcium phosphate," *Desalination and Water Treament* 111, 322-328. DOI: 10.5004/dwt.2018.22242

Essawy, H. A., Ghazy, M. B. M., El-Hai, F. A., and Mohamed, M. F. (2016). "Superabsorbent hydrogels via graft polymerization of acrylic acid from chitosan-cellulose hybrid and their potential in controlled release of soil nutrients," *International Journal of Biological Macromolecules* 89, 144-151. DOI: 10.1016/j.ijbiomac.2016.04.071

Filpponen, I., and Argyropoulos, D. S. (2010). "Regular linking of cellulose nanocrystals *via* click chemistry: Synthesis and formation of cellulose nanoplatelet gels," *Biomacromolecules* 11(4), 1060-1066. DOI: 10.1021/bm1000247

Fu, F., and Wang, Q. (2011). "Removal of heavy metal ions from wastewaters: A review," *Journal of Environmental Management* 92(3), 407-418. DOI: 10.1016/j.jenvman.2010.11.011

Gan, T., Zhang, Y., Su, Y., Hu, H., Huang, A., and Huang, Z., Chen, D., Yang, M., and Wu, J. (2017). "Esterification of bagasse cellulose with metal salts as efficient catalyst in mechanical activation-assisted solid phase reaction system," *Cellulose* 24(12), 5371-5387. DOI: 10.1007/s10570-017-1524-2

Gao, C., Zhang, X., Yuan, Y., Lei, Y., Gao, J., and Zhao, S. (2018). "Removal of

hexavalent chromium ions by core-shell sand/mg-layer double hydroxides (ldhs) in constructed rapid infiltration system," *Ecotoxicology and Environmental Safety* 166, 285-293. DOI: 10.1016/j.ecoenv.2018.09.083

Guo, Y., Wang, Z., Zhou, X., and Bai, R. (2016). "Removal of mercury (II) from aqueous solution with three commercial raw activated carbons," *Research on Chemical Intermediates* 43(4), 1-25. DOI: 10.1007/s11164-016-2761-y

Hadi, P., Xu, M., Ning, C., Carol, S. K. L., and Mckay, G. (2015). "A critical review on preparation, characterization and utilization of sludge-derived activated carbons for wastewater treatment'" *Chemical Engineering Journal* 260, 895-906. DOI: 10.1016/j.cej.2014.08.088

Ho, Y. S., and McKay, G. (1999). "Pseudo-second order model for sorption processes," *Process Biochemistry* 34(5), 451-465. DOI: 10.1016/S0032-9592(98)00112-5

Hoai, N. T., Yoo, D.-K., and Kim, D. (2010). "Batch and column separation characteristics of copper-imprinted porous polymer micro-beads synthesized by a direct imprinting method," *Journal of Hazardous Materials* 173(1-3), 462-467. DOI: 10.1016/j.jhazmat.2009.08.107

Hokkanen, S., Bhatnagar, A., and Sillanpaa, M. (2016). "A review on modification methods to cellulose-based adsorbents to improve adsorption capacity," *Water Research*, S0043135416300082. DOI: 10.1016/j.watres.2016.01.008

Hou, W. H., Zhou, J. S., Zhang, Y., Gao, X., Luo, Z. Y., and Cen, K. (2013). "Effect of H_2S on elemental mercury removal in coal gas by Fe_2O_3," *Proceedings of the CSEE* 33(23), 92-98.

Huang, X., Wang, A., Xu, X., Liu, H., and Shang, S. (2017). "Enhancement of hydrophobic properties of cellulose fibers via grafting with polymeric epoxidized soybean oil," *ACS Sustainable Chemistry & Engineering* 5(2), 1619-1627. DOI: 10.1021/acssuschemeng.6b02359

Jie, L., Yang, L., Yuejie, A., Ahmed, A., Tasawar, H., and Xiangke, W. (2018). "Combined experimental and theoretical investigation on selective removal of mercury ions by metal organic frameworks modified with thiol groups," *Chemical Engineering Journal*, S1385894718315080-. DOI: 10.1016/j.cej.2018.08.041

Kabdaşlı, I., Arslan, T., Ölmez-Hancı, T., Arslan-Alaton, I., and Tünay, O. (2009). "Complexing agent and heavy metal removals from metal plating effluent by electrocoagulation with stainless steel electrodes," *Journal of Hazardous Materials* 165(1-3), 838-845. DOI: 10.1016/j.jhazmat.2008.10.065

Kadirvelu, K., Thamaraiselvi, K., and Namasivayam, C. (2001). "Removal of heavy metals from industrial wastewaters by adsorption onto activated carbon prepared from an agricultural solid waste," *Bioresource Technology* 76(1), 63-65. DOI: 10.1016/S0960-8524(00)00072-9

Karatas, M., and Arslan, N. (2016). "Flow behaviours of cellulose and carboxymethyl cellulose from grapefruit peel," *Food Hydrocolloids* 58, 235-245. DOI: 10.1016/j.foodhyd.2016.02.035

Khan, S., Zhang, D., Yang, M. L., Yang, Y., He, H. Y., Jiang, H. (2017). "Removal of Cd by humic acid modified TiO_2 nanoparticles from aqueous solution," Desalination and Water Treatment 100, 193-203. DOI: 10.5004/dwt.2017.21802

Kheirandish, S., Ghaedi, M., Dashtian, K., Heidari, F., Pourebrahim, F., and Wang, S. (2017). "Chitosan extraction from lobster shells and its grafted with functionalized MWCNT for simultaneous removal of Pb^{2+}, ions and eriochrome cyanine R dye after

their complexation," *International Journal of Biological Macromolecules* 102, 181-191. DOI: 10.1016/j.ijbiomac.2017.03.035

Khoiruddin, Ariono, D., Subagjo, and Wenten, I. G. (2017). "Surface modification of ion-exchange membranes: Methods, characteristics, and performance," *Journal of Applied Polymer Science*, 45540. DOI: 10.1002/app.45540

Kim, U. J., Kuga, S., Wada, M., Okano, T., and Kondo, T. (2000). "Periodate oxidation of crystalline cellulose," *Biomacromolecules* 1(3), 488-492. DOI: 10.1021/bm0000337

Kim, U. J., Lee, Y. R., Kang, T. H., Choi, J. W., Kimura, S., and Wada, M. (2017). "Protein adsorption of dialdehyde cellulose-crosslinked chitosan with high amino group contents," *Carbohydrate Polymers* 163, 34-42. DOI: 10.1016/j.carbpol.2017.01.052

Konshina, D. N., Open'ko, Victor V., Temerdashev, Z. A., Gurinov, A. A., and Konshin, V. V. (2016). "Synthesis of novel silicagel-supported thiosemicarbazide and its properties for solid phase extraction of mercury," *Separation Science and Technology* 51(7), 1103-1111. DOI: 10.1080/01496395.2016.1143005

Koprivica, S., Siller, M., Hosoya, T., Roggenstein, W., Rosenau, T., and Potthast, A. (2016). "Regeneration of aqueous periodate solutions by ozone treatment: A sustainable approach for dialdehyde cellulose production," *ChemSusChem* 9(8), 825-833. DOI: 10.1002/cssc.201501639

Largitte, L., and Pasquier, R. (2016). "A review of the kinetics adsorption models and their application to the adsorption of lead by an activated carbon," *Chemical Engineering Research and Design*, S0263876216000691. DOI: 10.1016/j.cherd.2016.02.006

Lee, C. G., and Kim, S. B. (2016). "Cr(VI) adsorption to magnetic iron oxide nanoparticle-multi-walled carbon nanotube adsorbents," *Water Environment Research* 88(11), 2111-2120. DOI: 10.2175/106143016X14733681695401

Li, N., Chen, W., Chen, G., and Tian, J. (2017). "Rapid shape memory tempo-oxidized cellulose nanofibers/polyacrylamide/gelatin hydrogels with enhanced mechanical strength," *Carbohydrate Polymers* 171, 77-84. DOI: 10.1016/j.carbpol.2017.04.035

Li, Z. L., Meng, Z. R., and Yu, C. W. (2015). "Analysis of oxidized cellulose introduced into ramie fiber by oxidation degumming," *Textile Research Journal* 85(20), 2125-2135. DOI: 10.1177/0040517515581589

Lindh, E. L., Bergenstråhle-Wohlert, M., Terenzi, C., Salmén, L., and Furó, I. (2016). "Non-exchanging hydroxyl groups on the surface of cellulose fibrils: the role of interaction with water," *Carbohydrate Research* 434, 136-142. DOI: 10.1016/j.carres.2016.09.006

Liu, E. L., Xu, X. C., Zheng, X. D., Zhang, F. S. Liu, E. X., Li, C. X. (2017a). "An ion imprinted macroporous chitosan membrane for efficiently selective adsorption of dysprosium," *Separation and Purification Technology* 189, 288-295. DOI: 10.1016/j.seppur.2017.06.079

Liu, P., Wu, H., Yuan, N., Liu, Y., Pan, D., and Wu, W. (2017b). "Removal of U(VI) from aqueous solution using synthesized β-zeolite and its ethylenediamine derivative," *Journal of Molecular Liquids* 234, 40-48. DOI: 10.1016/j.molliq.2017.03.055

Lofrano, G., Carotenuto, M., Libralato, G., Domingos, R. F., Markus, A., Dini, L., Gautam, R. K., Baldantoni, D., Rossi, M., Sharma, S. K., *et al*. (2016). "Polymer functionalized nanocomposites for metals removal from water and wastewater: An

overview," *Water Research* 92, 22-37. DOI: 10.1016/j.watres.2016.01.033
Manasi, Vidya, R., and Rajesh, N. (2018). "Biosorption study of cadmium, lead and zinc ions onto halophilic bacteria and reduced graphene oxide," *Journal of Environmental Chemical Engineering*, S2213343718304214-. DOI: 10.1016/j.jece.2018.07.042
Micheau, C., Diat, O., and Bauduin, P. (2018). "Ion foam flotation of neodymium: From speciation to extraction," *Journal of Molecular Liquids* 253, 217-227. DOI: 10.1016/j.molliq.2018.01.022
Monier, M., and Abdel-Latif, D. A. (2012). "Preparation of cross-linked magnetic chitosan- phenylthiourea resin for adsorption of Hg(II), Cd(II) and Zn(II) ions from aqueous solutions," *Journal of Hazardous Materials* 209-210, 240-249. DOI: 10.1016/j.jhazmat.2012.01.015
Monier, M., and Abdel-Latif, D. A. (2013). "Modification and characterization of PET fibers for fast removal of Hg(II), Cu(II) and Co(II) metal ions from aqueous solutions," *Journal of Hazardous Materials* 250-251, 122-130. DOI: 10.1016/j.jhazmat.2013.01.056
Monier, M., Kenawy, I. M., and Hashem, M. A. (2014). "Synthesis and characterization of selective thiourea modified Hg(II) ion-imprinted cellulosic cotton fibers," *Carbohydrate Polymers* 106, 49-59. DOI: 10.1016/j.carbpol.2014.01.074
Morcali, M. H., Zeytuncu, B., Akman, S., and Yucel, O. (2015). "Preparation and sorption behavior of deae-cellulose-thiourea-glutaraldehyde sorbent for Pt(IV) and Pd(II) from leaching solutions," *Desalination and Water Treatment* 57(14), 6582-6593. DOI: 10.1080/19443994.2015.1010591
Motahari, S., Nodeh, M., and Maghsoudi, K. (2015). "Absorption of heavy metals using resorcinol formaldehyde aerogel modified with amine groups," *Desalination and Water Treatment* 57(36), 1-12. DOI: 10.1080/19443994.2015.1082506
Mousavi, S. J., Parvini, M., and Ghorbani, M. (2018). "Experimental design data for the zinc ions adsorption based on mesoporous modified chitosan using central composite design method," *Carbohydrate Polymers* 188, 197-212. DOI: 10.1016/j.carbpol.2018.01.105
Nayab, S., Farrukh, A., Oluz, Z., Tuncel, E., Tariq, S. R., ur Rahman, H., Kirchhoff, K., Duran, H., and Yameen, B. (2014). "Design and fabrication of branched polyamine functionalized mesoporous silica: An efficient absorbent for water remediation," *ACS Applied Materials & Interfaces* 6(6), 4408-4417. DOI: 10.1021/am500123k
Oehmen, A., Vergel, D., Fradinho, J., Reis, M. A., Crespo, J. G., and Velizarov, S. (2014). "Mercury removal from water streams through the ion exchange membrane bioreactor concept," *Journal of Hazardous Materials* 264(2), 65-70. DOI: 10.1016/j.jhazmat.2013.10.067
Oyetade, O. A., Skelton, A. A., Nyamori, V. O., Jonnalagadda, S. B., and Martincigh, B. S.. (2017). "Experimental and DFT studies on the selective adsorption of Pb^{2+}, and Zn^{2+}, from aqueous solution by nitrogen-functionalized multiwalled carbon nanotubes," *Separation and Purification Technology* 188, 174-187. DOI: 10.1016/j.seppur.2017.07.022
Park, J., and Lee, S. S. (2018). "Adsorption of mercury by activated carbon prepared from dried sewage sludge in simulated flue gas," *Journal of the Air & Waste Management Association* 68(10), 1077-1084. DOI: 10.1080/10962247.2018.1468364
Pourkarim, S., Ostovar, F., Mahdavianpour, M., and Moslemzadeh, M. (2017). "Adsorption of chromium(VI) from aqueous solution by artist's bracket fungi," *Separation Science & Technology 52*(1). DOI:

10.1080/01496395.2017.1299179

Qian, C., and Zhan, Q. (2016). "Bioremediation of heavy metal ions by phosphate-mineralization bacteria and its mechanism," *Journal of the Chinese Chemical Society* 63(7), 635-639. DOI: 10.1002/jccs.201600002

Salman, M., Athar, M., and Farooq, U. (2015). "Biosorption of heavy metals from aqueous solutions using indigenous and modified lignocellulosic materials," *Reviews in Environmental Science and Bio/Technology* 14(2), 211-228. DOI: 10.1007/s11157-015-9362-x

Sarkar, S., Sarkar, S., and Biswas, P. (2016). "Effective utilization of iron ore slime, a mining waste as adsorbent for removal of Pb(II) and Hg(II)," *Journal of Environmental Chemical Engineering* 5(1), 38-44. DOI: 10.1016/j.jece.2016.11.015

Segal, L., Creely, J. J., Martin, Jr., A. E., and Conrad, C. M. (1959). "An empirical method for estimating the degree of crystallinity of native cellulose using the X-ray diffractometer," *Textile Research Journal* 29(10), 786-794. DOI: 10.1177/004051755902901003

Senniappan, S., Palanisamy, S., Shanmugam, S., and Gobalsamy, S. (2016). "Adsorption of Pb(II) from aqueous solution by *Cassia fistula* seed carbon: Kinetics, equilibrium, and desorption studies," *Environmental Progress & Sustainable Energy* 36(1), 138-146. DOI: 10.1002/ep.12466

Siller, M., Amer, H., Bacher, M., Roggenstein, W., Rosenau, T., and Potthast, A. (2015). "Effects of periodate oxidation on cellulose polymorphs," *Cellulose* 22(4), 2245-2261. DOI: 10.1007/s10570-015-0648-5

Song, Z. Y., Feng, T., Hu, Y. M., Wang, L., and Zhang, X. Q. (2018). "Adsorption properties of graphene oxide/chitosan microspheres for removal of Cr(VI) from aqueous solutions," *Desalination and Water Treatment* 106, 191-199. DOI: 0.5004/dwt.2018.22039

Spinella, S., Maiorana, A., Qian, Q., Dawson, N. J., Hepworth, V., McCallum, S. A., Ganesh, M., Singer, K. D., and Gross, R. A. (2016). "Concurrent cellulose hydrolysis and esterificationto prepare a surface-modified cellulose nanocrystal decorated withcarboxylic acid moieties," *ACS Sustainable Chemistry & Engineering* 4(3), 1538-1550. DOI: 10.1021/acssuschemeng.5b01489

Su, Y., Cui, M., Zhu, J., Wu, Y., Wei, Y., and Bian, S. (2017). "A facile synthesis of nanosheet-structured barium carbonate spheres with a superior adsorption capacity for Cr(VI) removal," *Journal of Materials Science* 53(6), 4018-4088. DOI: 10.1007/s10853-017-1861-4

Sun, L. J., Qian, X. R., Ding, C. Y., and An, X. H. (2018a). "Integration of graft copolymerization and ring-opening reaction: A mild and effective preparation strategy for "clickable" cellulose fibers," *Carbohydrate Polymers* 198, 41-50. DOI: 10.1016/j.carbpol.2018.06.054

Sun, N., Wen, X., and Yan, C. (2018b). "Adsorption of mercury ions from wastewater aqueous solution by amide functionalized cellulose from sugarcane bagasse," *International Journal of Biological Macromolecules* 108, 1199-1206. DOI: 10.1016/j.ijbiomac.2017.11.027

Taoufik, F., El Hadek, M., Hnini, M. C., Benchanaa, M'Barek, El Hammioui, M., and Hassani, L. M. I. (2017). "Sorption isotherms and isosteric heats of sorption of mint variety (*Mentha viridis*) leaves and stems: experimental and mathematical investigations," *The European Physical Journal Special Topics* 226(5), 993-1000. DOI: 10.1140/epjst/e2016-60180-1

Terdputtakun, A., Arqueropanyo, O. A., Sooksamiti, P., Janhom, S., and Naksata, W. (2017). "Adsorption isotherm models and error analysis for single and binary adsorption of Cd(II) and Zn(II) using leonardite as adsorbent," *Environmental Earth Sciences* 76(22), 777. DOI: 10.1007/s12665-017-7110-y

Tian, X., and Jiang, X. (2017). "Preparing water-soluble 2, 3-dialdehyde cellulose as a bio-origin cross-linker of chitosan," *Cellulose* 25(2), 987-998. DOI: 10.1007/s10570-017-1607-0

Tian, Y., Wu, M., Liu, R., Li, Y., Wang, D., Tan, J., Wu, R., and Huang, Y. (2011a). "Electrospun membrane of cellulose acetate for heavy metal ion adsorption in water treatment," *Carbohydrate Polymers* 83(2), 743-748. DOI: 10.1016/j.carbpol.2010.08.054

Tian, Y., Wu, M., Lin, X., Huang, P., and Huang, Y. (2011b). "Synthesis of magnetic wheat straw for arsenic adsorption," *Journal of Hazardous Materials* 193, 10-16. DOI: 10.1016/j.jhazmat.2011.04.093

Toba, K., Yamamoto, H., and Yoshida, M. (2013). "Crystallization of cellulose microfibrils in wood cell wall by repeated dry-and-wet treatment, using x-ray diffraction technique," *Cellulose* 20(2), 633-643. DOI: 10.1007/s10570-012-9853-7

Veelaert, S., De Wit, D., Gotlieb, K. F., and Verhé, R. (1997). "Chemical and physical transitions of periodate oxidized potato starch in water," *Carbohydrate Polymers* 33(2-3), 153-162. DOI: 10.1016/S0144-8617(97)00046-5

Wang, N., Jin, R. N., Omer, A. M., and Ouyang, X. K. (2017). "Adsorption of Pb(II) from fish sauce using carboxylated cellulose nanocrystal: isotherm, kinetics, and thermodynamic studies," *International Journal of Biological Macromolecules*102, 232-240. DOI: 10.1016/j.ijbiomac.2017.03.150

Wang, Y. G., Shi, L., Gao, L., Wei, Q., Cui, L. M., Hu, L. H., Yan, L. G., and Du, B. (2015). "The removal of lead ions from aqueous solution by using magnetic hydroxypropyl chitosan/oxidized multiwalled carbon nanotubes composites," *Journal of Colloid and Interface Science* 451, 7-14. DOI:10.1016/j.jcis.2015.03.048

Wu, S., Wang, F., Yuan, H., Zhang, L., Mao, S., and Liu, X., *et al*. (2018). "Fabrication of xanthate-modified chitosan/poly(n-isopropylacrylamide) composite hydrogel for the selective adsorption of Cu(II), Pb(II) and Ni(II) metal ions," *Chemical Engineering Research and Design* 139, 197-210. DOI: 10.1016/j.cherd.2018.09.035

Xia, Z., Baird, L., Zimmerman, N., and Yeager, M. (2017). "Heavy metal ion removal by thiol functionalized aluminum oxide hydroxide nanowhiskers," *Applied Surface Science* 416, 565-573. DOI: 10.1016/j.apsusc.2017.04.095

Xu, L., Tian, J., Wu, H., Lu, Z., and Hu, Y. (2017). "Effect of Pb^{2+} ions on ilmenite flotation and adsorption of benzohydroxamic acid as a collector," *Applied Surface Science* 425. DOI: 10.1016/j.apsusc.2017.07.123

Yan, H., Li, H., Tao, X., Li, K., Yang, H., Li, A., Xiao, S., and Cheng, R. (2014). "Rapid removal and separation of iron(II) and manganese(II) from micropolluted water using magnetic graphene oxide," *ACS Applied Materials & Interfaces* 6(12), 9871-9880. DOI: 10.1021/am502377n

Yang, L., Tang, C., Ahmad, M., Yaroshchuk, A., and Bruening, M. L. (2018). "High selectivities among monovalent cations in dialysis through cation exchange membranes coated with polyelectrolyte multilayers," *ACS Applied Materials & Interfaces* 10(50), 44134-44143. DOI: 10.1021/acsami.8b16434

Yang, H., Chen, D., and van de Ven, T. G. M. (2015). "Preparation and characterization

of sterically stabilized nanocrystalline cellulose obtained by periodate oxidation of cellulose fibers," *Cellulose* 22(3), 1743-1752. DOI: 10.1007/s10570-015-0584-4

Yao, C. (2000). "Extended and improved Langmuir equation for correlating adsorption equilibrium data," *Separation and Purification Technology* 19(3), 237-242. DOI: 10.1016/S1383-5866(00)00060-5

Yao, X., Wang, H., Ma, Z., Liu, M., Zhao, X., and Jia, D. (2016). "Adsorption of Hg(II) from aqueous solution using thiourea functionalized chelating fiber," *Chinese Journal of Chemical Engineering* 24(10), 1344-1352. DOI: 10.1016/j.cjche.2016.07.008

Yenial, Ü., and Bulut, G. (2017). "Examination of flotation behavior of metal ions for process water remediation," *Journal of Molecular Liquids* 241, 130-135. DOI: 10.1016/j.molliq.2017.06.011

Yusuf, U., and Tekin, S. (2017). "Optimization with response surface methodology of biosorption conditions of Hg(II) ions from aqueous media by *Polyporus squamosus* fungi as a new biosorbent," *Archives of Environmental Protecton* 43(2), 37-43. DOI: 10.1515/aep-2017-0015

Yu, J. G., Yu, L. Y., Yang, H., Liu, Q., Chen, X. H., Jiang, X. Y., *et al*. (2015). "Graphene nanosheets as novel adsorbents in adsorption, preconcentration and removal of gases, organic compounds and metal ions," *Science of The Total Environment* 502, 70-79. DOI:10.1016/j.scitotenv.2014.08.077

Zhang, D., Yin, Y., and Liu, J. (2017). "Removal of Hg^{2+} and methylmercury in waters by functionalized multi-walled carbon nanotubes: Adsorption behavior and the impacts of some environmentally relevant factors," *Chemical Speciation & Bioavailability 29*(1), 161-169. DOI: 10.1080/09542299.2017.1378596

Zhang, Z., Zheng, H., Sun, Y., Zhao, C., Zhou, Y., and Tang, X. (2016). "A combined process of chemical precipitation and flocculation for treating phosphating wastewater," *Desalination and Water Treatment*, 1-12. DOI:10.1080/19443994.2016.1157707

Zhao, L., Xu, L., Wu, X., Zhao, G., Jiao, L., and Chen, J. (2018). "Characteristics and sources of mercury in precipitation collected at the urban, suburban and rural sites in a city of southeast China," *Atmospheric Research* S0169809518301741. DOI: 10.1016/j.atmosres.2018.04.019

Zhu, F., Li, L., and Xing, J. (2017). "Selective adsorption behavior of Cd(II) ion imprinted polymers synthesized by microwave-assisted inverse emulsion polymerization: adsorption performance and mechanism," *Journal of Hazardous Materials* 321, 103-110. DOI: 10.1016/j.jhazmat.2016.09.012

Zou, H., Lv, P. F., Wang, X., Wu, D., and Yu, D. G. (2017). "Electrospun poly(2-aminothiazole)/cellulose acetate fiber membrane for removing Hg(II) from water," *Journal of Applied Polymer Science* 134(21). DOI: 10.1002/app.44879

Article submitted: January 10, 2019; Peer review completed: March 29, 2019; Revised version received: April 20, 2019; Accepted: April 22, 2019; Published: April
DOI: 4670-4695